

*Journal of Organometallic Chemistry*, 370 (1989) 263–276  
Elsevier Sequoia S.A., Lausanne – Printed in The Netherlands  
JOM 09756

## Catalytic and structural studies of $Rh^I$ complexes of (–)-(2*S*,4*S*)-2,4-bis(diphenylphosphino)pentane. Asymmetric hydrogenation of acetophenonebenzylimine and acetophenone

**J. Bakos, I. Tóth, B. Heil**

*Institute of Organic Chemistry, University of Chemical Engineering, H-8201 Veszprém,  
P.O. Box 158 (Hungary)*

**G. Szalontai**

*Research Institute for Heavy Chemical Industries, H-8200 Veszprém, P.O. Box 160 (Hungary)*

**L. Párkányi and V. Fülöp**

*Central Research Institute for Chemistry, Hungarian Academy of Sciences, H-1525 Budapest,  
P.O. Box 17 (Hungary)*

(Received October 24th, 1988)

### Abstract

Rhodium(I) complexes formed by (–)-(2*S*,4*S*)-2,4-bis(diphenylphosphino)pentane (BDPP) are efficient catalysts for the hydrogenation of acetophenone and acetophenonebenzylimine. The composition of the solvent mixture and the reaction temperature have a marked influence on the enantioselectivity. These effects are thought to be related to the enhanced conformational flexibility of six-membered rings when simple substrates without functional groups are coordinated to the rhodium. X-ray crystallographic studies reveal that in  $[Rh((S,S)\text{-BDPP})NBD]^+$  (1) the ligand is in a chair conformation, and that in  $[Rh((S,S)\text{-BDPP})COD]^+$  (2) the chelate ring is in a  $\delta$ -skew conformation. Studies of  $Rh((S,S)\text{-BDPP})(NBD)Cl$  (3) in solution indicate a trigonal bipyramidal structure with a chair conformation of the ring in aromatic solvents and a conformationally labile ring in methanol.

---

### Introduction

The efficiency of rhodium(I) catalysts modified by the enantiomers of 2,4-bis(diphenylphosphino)pentane have been demonstrated in asymmetric hydrogenation of (*Z*)- $\alpha$ -(acylamido)acrylic acids [1,3],  $\alpha$ -ethylstyrene, acetophenone, acetophenonebenzylimine [3], and in asymmetric hydroformylation of some prochiral olefins [4]. Bosnich et al. emphasized the importance of chiral conformations stabilized by

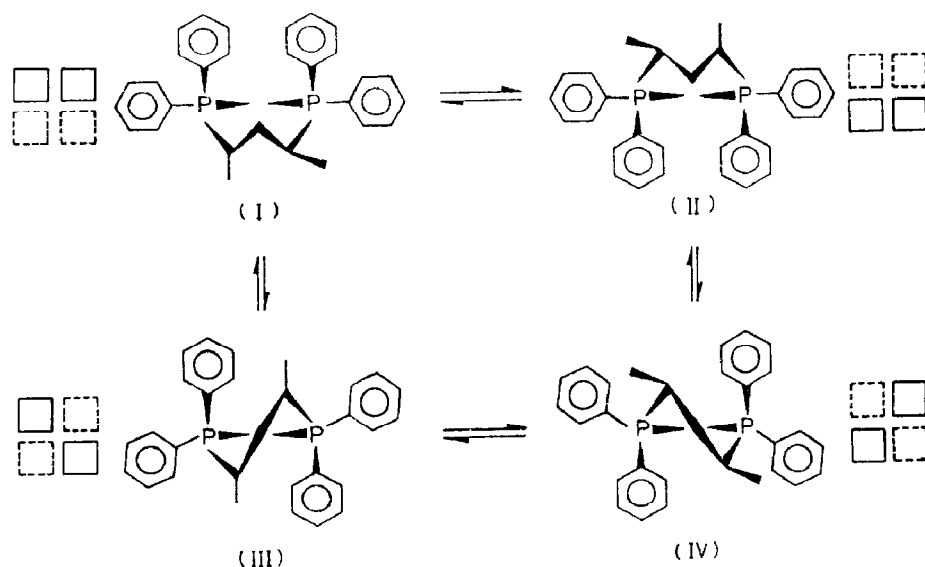


Fig. 1. Some possible conformations of the chelate ring with  $(S,S)$ -BDPP ( $\square$  crowded space,  $\square$  free space).

chiral centers at the ring backbone [5,6]. Furthermore, the skew conformation of the chelate ring in the  $\text{BDPP}^*$  complexes is assumed to be predominant [1], since the chair conformation itself is achiral, and the phenyl groups are not in a chiral array.

As the stereochemistry of the phosphine ligand plays a major role in determining the enantioselectivity as well as the efficiency of the catalytic action, we decided to examine the solid and solution structures of these complexes incorporating BDPP, and to relate the results obtained in asymmetric hydrogenation of acetophenone, acetophenonebenzylimine, and in asymmetric hydroformylation of styrene to the conformation of the chelate ring.

## Results and discussion

The conformation of a six-membered chelate ring containing  $(S,S)$ -BDPP is not obvious, because the preference of a chair form for the chelate ring and the equatorial preference of methyl groups compete with each other. Four conformers are conceivable for a coordinated  $(S,S)$ -BDPP (Fig. 1). The two skew conformers are energetically not equivalent. Structure **III** is destabilized by the skew conformation and the two axial methyl substituents. But the  $\delta$ -skew conformer (**IV**) is favoured by the presence of two equatorial methyl groups. The chair forms, **I** and **II**, being identical, are energetically equivalent, but, are destabilized by the axial methyl group, which may interact sterically with the apical ligands. According to the experimental [7–10] and theoretical data [11,12] the skew conformation having two equatorial methyl group is preferred.

The availability of two conformations for the ring is evident from the X-ray crystal structure determinations.

\* Bosnich's group [1] has termed this compound skewphos, but as in our earlier publication [2] the abbreviation BDPP is used here.

Table 1

Atomic coordinate and thermal parameters of **1**, with e.s.d.'s in parentheses

Atom	<i>x</i>	<i>y</i>	<i>z</i>	<i>B</i> <sub>eq</sub>
Rh	0.06974(2)	0.0	0.47909(2)	2.387(4)
P(1)	0.0597(1)	0.06472(6)	0.2807(1)	2.41(2)
P(2)	0.2506(1)	0.07305(6)	0.6545(1)	2.58(2)
C(1)	0.2252(5)	0.1559(3)	0.1832(5)	4.2(1)
C(2)	0.2338(4)	0.1129(2)	0.3150(4)	3.0(1)
C(3)	0.2851(4)	0.1623(2)	0.4504(4)	3.0(1)
C(4)	0.3768(4)	0.1262(2)	0.6037(4)	3.4(1)
C(5)	0.5113(5)	0.0845(3)	0.6132(5)	4.7(1)
C(6)	-0.1626(5)	-0.0636(3)	0.5164(5)	3.5(1)
C(7)	-0.1601(5)	-0.1478(3)	0.5029(5)	4.3(1)
C(8)	-0.0201(5)	-0.1468(2)	0.4793(4)	3.4(1)
C(9a)	-0.0035(5)	-0.0496(2)	0.6324(4)	3.3(1)
C(9b)	0.0835(5)	-0.1004(2)	0.6111(4)	3.8(1)
C(10a)	-0.1564(5)	-0.0427(2)	0.3725(5)	4.7(1)
C(10b)	-0.0684(5)	-0.0933(2)	0.3516(4)	3.3(1)
C(11)	0.0270(3)	0.0009(3)	0.1311(2)	2.69(7)
C(12)	0.1466(4)	-0.0408(2)	0.1404(5)	3.4(1)
C(13)	0.1248(5)	-0.0966(3)	0.0402(5)	3.7(1)
C(14)	-0.0158(6)	-0.1104(3)	-0.0699(4)	3.8(1)
C(15)	-0.1355(5)	-0.0704(3)	-0.0818(4)	4.4(1)
C(16)	-0.1139(4)	-0.0150(2)	0.0188(3)	3.4(1)
C(21)	-0.0886(4)	0.1323(2)	0.1980(4)	3.0(1)
C(22)	-0.1376(5)	0.1576(3)	0.0549(5)	3.8(1)
C(23)	-0.2480(6)	0.2101(3)	-0.0034(5)	5.3(1)
C(24)	-0.3105(6)	0.2370(3)	0.0788(6)	5.8(1)
C(25)	-0.2644(6)	0.2139(3)	0.2230(6)	5.2(1)
C(26)	-0.1531(5)	0.1606(3)	0.2811(4)	3.9(1)
C(31)	0.1652(4)	0.1432(2)	0.7208(4)	2.89(9)
C(32)	0.0149(4)	0.1388(2)	0.6806(4)	3.0(1)
C(33)	-0.0533(5)	0.1902(3)	0.7293(4)	3.5(1)
C(34)	0.0286(5)	0.2459(2)	0.8206(4)	3.5(1)
C(35)	0.1772(6)	0.2507(2)	0.8621(5)	4.2(1)
C(36)	0.2470(5)	0.1998(2)	0.8133(4)	3.7(1)
C(41)	0.3685(4)	0.0204(2)	0.8176(4)	3.2(1)
C(42)	0.3884(5)	0.0358(3)	0.9593(5)	4.0(1)
C(43)	0.4684(5)	-0.0132(4)	1.0749(4)	5.3(1)
C(44)	0.5268(5)	-0.0752(3)	1.0513(5)	5.9(1)
C(45)	0.5115(5)	-0.0906(3)	0.9131(6)	5.3(1)
C(46)	0.4333(5)	-0.0429(2)	0.7975(5)	4.1(1)
Cl	0.5684(1)	0.33747(8)	0.5333(1)	5.02(3)
O(1)	0.5339(7)	0.4089(4)	0.5638(7)	13.5(2)
O(2)	0.7055(4)	0.3491(4)	0.5407(5)	10.6(2)
O(3)	0.4539(5)	0.3244(3)	0.3937(5)	11.1(2)
O(4)	0.5630(5)	0.2925(3)	0.6412(5)	10.5(1)

The atomic coordinates are listed in Tables 1 and 3, and selected bond lengths and bond angles in Tables 2 and 4. The six-membered chelate ring in **1** has a chair conformation, with the phenyl rings in achiral arrangement (Fig. 2). The mirror symmetry for the phenyl ipso atoms (C(21), C(31) in axial, C(11), C(41) in equatorial positions) is fairly well satisfied, as shown by the torsion angles:

Table 2

Selected bond lengths (Å) and bond angles (°) of **1** with e.s.d.'s in parentheses

<i>Bond lengths</i>					
Rh–P(1)	2.302(1)	P(2)–C(4)	1.851(4)	C(6)–C(10a)	1.541(7)
Rh–P(2)	2.305(1)	P(2)–C(31)	1.836(4)	C(7)–C(8)	1.534(5)
Rh–C(9a)	2.202(4)	P(2)–C(41)	1.812(4)	C(8)–C(9b)	1.525(6)
Rh–C(9b)	2.242(5)	C(1)–C(2)	1.522(6)	C(8)–C(10b)	1.518(6)
Rh–C(10a)	2.171(4)	C(2)–C(3)	1.527(6)	C(9a)–C(9b)	1.361(6)
Rh–C(10b)	2.209(4)	C(3)–C(4)	1.551(6)	C(10a)–C(10b)	1.363(6)
P(1)–C(2)	1.847(3)	C(4)–C(5)	1.519(5)	Cl–O(1)	1.423(7)
P(1)–C(11)	1.825(5)	C(6)–C(7)	1.547(8)	Cl–O(2)	1.364(2)
P(1)–C(21)	1.822(4)	C(6)–C(9a)	1.515(5)	Cl–O(3)	1.380(5)
				Cl–O(4)	1.394(5)
<i>Bond angles</i>					
P(1)–Rh–P(2)	94.7(1)	C(1)–C(2)–C(3)		110.3(6)	
P(1)–Rh–C(10a)	97.6(2)	C(2)–C(3)–C(4)		117.0(6)	
P(1)–Rh–C(10b)	96.9(2)	P(2)–C(4)–C(3)		109.6(5)	
P(2)–Rh–C(9a)	95.3(2)	P(2)–C(4)–C(5)		115.1(5)	
P(2)–Rh–C(9b)	101.6(2)	C(3)–C(4)–C(5)		112.4(6)	
Rh–P(1)–C(2)	115.0(2)	C(7)–C(6)–C(9a)		100.6(6)	
Rh–P(1)–C(11)	108.7(2)	C(7)–C(6)–C(10a)		98.8(6)	
Rh–P(1)–C(21)	116.9(2)	C(9a)–C(6)–C(10a)		102.1(6)	
C(2)–P(1)–C(11)	104.8(3)	C(6)–C(7)–C(8)		93.2(6)	
C(2)–P(1)–C(21)	105.7(3)	C(7)–C(8)–C(9b)		100.2(6)	
C(11)–P(1)–C(21)	104.6(3)	C(7)–C(8)–C(10b)		100.6(6)	
Rh–P(2)–C(4)	119.3(2)	C(9b)–C(8)–C(10b)		102.5(6)	
Rh–P(2)–C(31)	110.6(2)	C(6)–C(9a)–C(9b)		106.7(6)	
Rh–P(2)–C(41)	110.8(2)	C(8)–C(9b)–C(9a)		106.8(6)	
C(4)–P(2)–C(31)	103.4(3)	C(6)–C(10a)–C(10b)		107.0(7)	
C(4)–P(2)–C(41)	106.8(3)	C(8)–C(10b)–C(10a)		106.3(6)	
C(31)–P(2)–C(41)	104.8(3)	O(1)–Cl–O(2)		100.8(6)	
P(1)–C(2)–C(1)	114.4(5)	O(1)–Cl–O(3)		102.2(6)	
P(1)–C(2)–C(3)	110.7(5)	O(1)–Cl–O(4)		105.6(6)	
		O(2)–Cl–O(3)		115.6(6)	
		O(2)–Cl–O(4)		116.9(6)	
		O(3)–Cl–O(4)		113.1(5)	

C(3)–C(2)–P(1)–C(11):  $-174^\circ$ , C(3)–C(4)–P(2)–C(41):  $170^\circ$ , C(3)–C(2)–P(1)–C(21):  $76^\circ$ , C(3)–C(4)–P(2)–C(31):  $-79^\circ$ .

The asymmetric unit of the [Rh((*S,S*)-BDPP)COD]ClO<sub>4</sub> (**2**) complex contains two non-equivalent molecules with different orientations of the COD (Fig. 3). Both of them have a twofold axis which goes through Rh and C(3). The asymmetric unit contains halves of two independent cations and one perchlorate anion in a general position. The six-membered chelate ring adopts  $\delta$ -skew conformation (**IV**) with equatorial methyl groups in both cations, and the COD parts of the cations are in quasi enantiomerically-related positions, so that the endocyclic torsion angles are identical pairwise with opposite signs (Table 5). The phenyl rings are in a chiral array with alternating quasi-axial and quasi-equatorial positions.

By far the most studied catalytic asymmetric reaction is the hydrogenation of enamides to give amino acid derivatives, and relatively few results have appeared on the enantioselective hydrogenation of Schiff bases and ketones [13–15]. Earlier

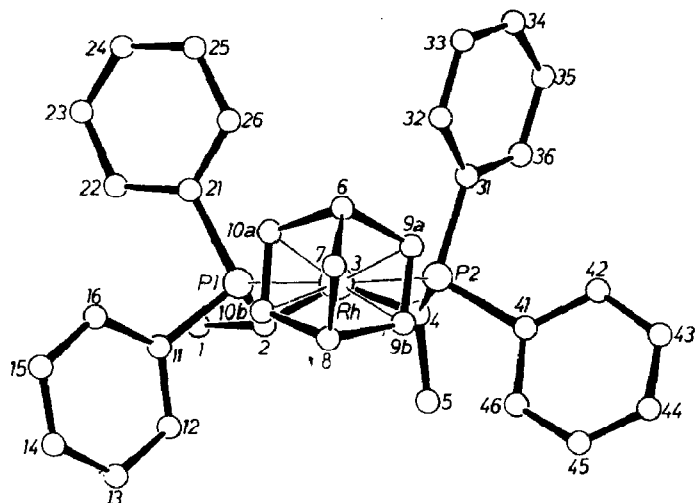


Fig. 2. Perspective view of  $[\text{Rh}((S,S)\text{-BDPP})\text{NBD}]^+$  (**1**) with the atom-numbering scheme.

studies of hydrogenation of enamide involving use of BDPP have shown that the catalyst is insensitive to the reaction temperature and the solvent [1,3].

For the hydrogenation of acetophenonebenzylimine and acetophenone an “in situ” catalyst ( $[\text{Rh}(\text{diene})\text{Cl}]_2 + \text{BDPP}$ ) was used, and a strong dependence of the e.e. on the solvent composition was observed (Table 6 and 7, Fig. 4). Increase in the ratio of  $\text{C}_6\text{H}_6/\text{MeOH}$  is accompanied by a large fall in the catalytic activity, and in the case of the Schiff base there is a reversal of the stereoselectivity. The rate of the hydrogenation followed by the formation of the amine or alcohol, was about 30 times larger for acetophenonebenzylimine, and about 3 times larger for acetophenone, in methanol than in benzene. It should be noted that “in situ” prepared catalysts and the cationic complexes gave the same optical yields in methanol.

The  $^{31}\text{P}$  NMR spectrum of  $\text{Rh}(\text{NBD})(S,S\text{-BDPP})\text{Cl}$  recorded in  $\text{CO}_3\text{OD}$  shows a sharp doublet ( $^1J(\text{RhP})$  149 Hz) at 29 ppm. The same value was obtained for **1** and **2** in  $\text{CD}_3\text{OD}$ , and is characteristic of a square planar structure (**3a**, Fig. 5). However, in benzene or toluene at 309 K the spectrum displays two doublets; indicating the

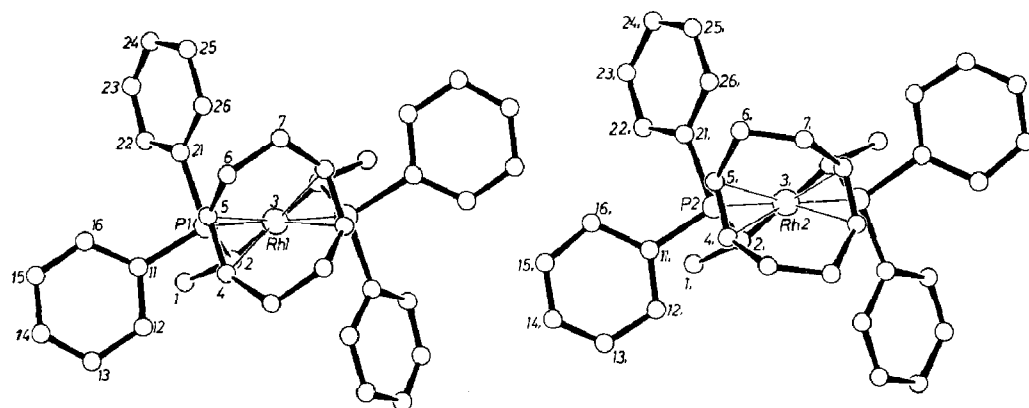


Fig. 3. Perspective view of  $[\text{Rh}((S,S)\text{-BDPP})\text{COD}]^+$  (**2**) with the atom-numbering scheme.

Table 3

Atomic coordinate and thermal parameters of **2** with e.s.d.'s in parentheses

Atom	<i>x</i>	<i>y</i>	<i>z</i>	<i>B</i> <sub>eq</sub>	
Rh(1)	0.0	0.0	0.0	2.22(1)	Mult = 0.50
P(1)	-0.06635(8)	0.1199(1)	0.04881(6)	2.56(3)	
C(1)	-0.1636(5)	0.3048(5)	0.0125(4)	4.8(2)	
C(2)	-0.0920(4)	0.2346(4)	-0.0034(3)	3.5(1)	
C(3)	0.0	0.2951(7)	0.0	3.9(2)	Mult = 0.50
C(4)	-0.1161(4)	-0.1066(4)	-0.0106(3)	3.6(1)	
C(5)	-0.0495(4)	-0.1187(4)	0.0567(2)	3.0(1)	
C(6)	0.0267(5)	-0.1992(5)	0.0799(4)	5.3(2)	
C(7)	0.1225(4)	-0.1713(6)	0.0732(4)	4.7(2)	
C(11)	-0.1806(3)	0.0925(4)	0.0619(2)	2.9(1)	
C(12)	-0.2635(3)	0.0874(4)	0.0021(3)	3.7(1)	
C(13)	-0.3543(4)	0.0644(5)	0.0090(4)	4.7(2)	
C(14)	-0.3577(4)	0.0504(6)	0.0735(4)	5.2(2)	
C(15)	-0.2781(4)	0.0541(7)	0.1322(3)	4.8(2)	
C(16)	-0.1886(4)	0.0743(5)	0.1266(3)	4.0(1)	
C(21)	-0.0171(4)	0.1491(5)	0.1362(3)	3.8(1)	
C(22)	0.0049(6)	0.2275(6)	0.1746(4)	6.6(2)	
C(23)	0.0720(7)	0.2496(9)	0.2351(5)	10.6(3)	
C(24)	0.1529(7)	0.197(1)	0.2635(4)	11.7(4)	
C(25)	0.1713(5)	0.1184(9)	0.2277(4)	7.1(3)	
C(26)	0.1030(5)	0.0973(7)	0.1623(3)	5.3(2)	
Rh(2)	0.5	-0.01893(4)	0.5	2.54(1)	Mult = 0.50
P(2)	0.38719(8)	-0.1392(1)	0.49084(7)	2.70(3)	
C(1,)	0.3728(4)	-0.3228(5)	0.5556(3)	4.2(1)	
C(2,)	0.4417(4)	-0.2523(4)	0.5372(3)	3.2(1)	
C(3,)	0.5	-0.3040(6)	0.5	3.3(2)	Mult = 0.50
C(4,)	0.4194(4)	0.1009(4)	0.5305(3)	3.5(1)	
C(5,)	0.3832(3)	0.0928(4)	0.4620(3)	3.8(1)	
C(6,)	0.4067(5)	0.1545(5)	0.4081(4)	5.0(1)	
C(7,)	0.5099(5)	0.1795(5)	0.4284(3)	4.4(1)	
C(11,)	0.2979(3)	-0.1055(4)	0.5311(3)	3.0(1)	
C(12,)	0.3264(5)	-0.0902(5)	0.6013(3)	4.2(1)	
C(13,)	0.2583(6)	-0.0656(6)	0.6327(4)	5.2(2)	
C(14,)	0.1669(5)	-0.0521(6)	0.5953(4)	5.9(2)	
C(15,)	0.1368(5)	-0.0640(7)	0.5227(5)	5.8(2)	
C(16,)	0.1994(4)	-0.0943(5)	0.4900(4)	4.3(2)	
C(21,)	0.3211(3)	-0.1769(4)	0.4013(3)	3.4(1)	
C(22,)	0.2518(5)	-0.2503(5)	0.3859(3)	5.0(2)	
C(23,)	0.2097(7)	-0.2819(7)	0.3159(5)	7.7(2)	
C(24,)	0.2335(7)	-0.2423(7)	0.2638(4)	6.4(2)	
C(25,)	0.2980(6)	-0.1658(7)	0.2781(3)	5.9(2)	
C(26,)	0.3435(4)	-0.1345(6)	0.3456(3)	4.2(1)	
Cl	0.4558(1)	0.0375(1)	0.2081(1)	6.03(6)	
O(1)	0.532(1)	-0.012(1)	0.1920(7)	20.5(8)	
O(2)	0.367(1)	0.007(1)	0.1699(6)	23.3(6)	
O(3)	0.468(1)	0.122(1)	0.1843(7)	17.9(6)	
O(4)	0.4746(9)	0.033(1)	0.2763(4)	17.0(7)	

presence of two different phosphorus atoms, and so a trigonal bipyramidal structure (**3b**). When the spectrum was recorded in CD<sub>2</sub>Cl<sub>2</sub> this eight-line pattern was apparent at 195 K. At room temperature there is only a sharp doublet (25.3 ppm,

Table 4

Selected bond lengths (Å) and bond angles of **2** with e.s.d.'s in parentheses

<i>Bond lengths</i>					
Rh(1)–P(1)	2.300(1)	C(4)–C(7 <sup>*</sup> ) <sup>a</sup>	1.522(10)	C(1,)–C(2,)	1.535(8)
Rh(1)–C(4)	2.204(5)	C(5)–C(6)	1.529(9)	C(2,)–C(3,)	1.497(6)
Rh(1)–C(5)	2.251(5)	C(6)–C(7)	1.510(7)	C(4,)–C(5,)	1.305(10)
P(1)–C(2)	1.861(6)	Rh(2)–P(2)	2.303(1)	C(4,)–C(7, <sup>*</sup> )	1.533(9)
P(1)–C(11)	1.828(4)	Rh(2)–C(4,)	2.233(5)	C(5,)–C(6,)	1.509(9)
P(1)–C(21)	1.816(6)	Rh(2)–C(5,)	2.234(5)	C(6,)–C(7,)	1.472(8)
C(1)–C(2)	1.540(8)	P(2)–C(2,)	1.850(6)	Cl–O(1)	1.441(14)
C(2)–C(3)	1.569(7)	P(2)–C(11,)	1.824(4)	Cl–O(2)	1.335(13)
C(4)–C(5)	1.387(8)	P(2)–C(21,)	1.811(6)	Cl–O(3)	1.285(16)
				Cl–O(4)	1.310(9)
<i>Bond angles</i>					
P(1)–Rh(1)–C(4)	95.1(3)	P(2)–Rh(2)–C(4,)	96.6(3)		
P(1)–Rh(1)–C(5)	92.4(2)	P(2)–Rh(2)–C(5,)	90.9(3)		
P(1)–Rh(1)–P(1 <sup>*</sup> )	88.6(1)	P(2)–Rh(2)–P(2 <sup>*</sup> )	88.4(1)		
Rh(1)–P(1)–C(2)	113.4(3)	Rh(2)–P(2)–C(2,)	112.7(3)		
Rh(1)–P(1)–C(11)	117.4(3)	Rh(2)–P(2)–C(11,)	113.0(3)		
Rh(1)–P(1)–C(21)	109.2(3)	Rh(2)–P(2)–C(21,)	114.3(3)		
C(2)–P(1)–C(11)	103.7(4)	C(2,)–P(2)–C(11,)	104.0(4)		
C(2)–P(1)–C(21)	107.6(5)	C(2,)–P(2)–C(21,)	104.9(4)		
C(11)–P(1)–C(21)	104.8(4)	C(11,)–P(2)–C(21,)	107.1(4)		
P(1)–C(2)–C(1)	115.6(7)	P(2)–C(2,)–C(1,)	116.3(7)		
P(1)–C(2)–C(3)	114.7(7)	P(2)–C(2,)–C(3,)	111.6(6)		
C(1)–C(2)–C(3)	107.5(8)	C(1,)–C(2,)–C(3,)	111.1(8)		
C(2)–C(3)–C(2 <sup>*</sup> )	116.1(8)	C(2,)–C(3,)–C(2, <sup>*</sup> )	123.4(8)		
C(5)–C(4)–C(7 <sup>*</sup> )	124.5(9)	C(5,)–C(4,)–C(7, <sup>*</sup> )	126.2(9)		
C(4)–C(5)–C(6)	125.8(9)	C(4,)–C(5,)–C(6,)	127.2(10)		
C(5)–C(6)–C(7)	113.5(10)	C(5,)–C(6,)–C(7,)	113.5(10)		
C(6)–C(7)–C(4 <sup>*</sup> )	115.3(10)	C(6,)–C(7,)–C(4, <sup>*</sup> )	115.5(10)		
O(1)–Cl(1)–O(2)	114.0(16)	O(2)–Cl–O(3)	107.4(16)		
O(1)–Cl–O(3)	96.7(16)	O(2)–Cl–O(4)	114.0(17)		
O(1)–Cl–O(4)	108.4(17)	O(3)–Cl–O(4)	115.3(17)		

<sup>a</sup> \* indicates atoms related by crystallographic twofold axes.

<sup>1</sup>J(RhP) 133 Hz). This behaviour could be attributed to existence of an equilibrium between trigonal-bipyramidal or trigonal-bipyramidal and square-pyramidal (**3c**) forms.

When the spectra were recorded in benzene/methanol mixtures with varying ratios of the two components, a linear dependence of <sup>1</sup>J(RhP) on the solvent

Table 5

Endocyclic torsion angles for COD <sup>a</sup>

C(4)–C(5)–C(6)–C(7)	91.4	C(6,)–C(7,)–C(4, <sup>*</sup> )–C(5, <sup>*</sup> )	–92.3
C(5)–C(6)–C(7)–C(4 <sup>*</sup> )	–35.3	C(5,)–C(6,)–C(7,)–C(4, <sup>*</sup> )	34.9
C(6)–C(7)–C(4 <sup>*</sup> )–C(5 <sup>*</sup> )	–41.9	C(4,)–C(5,)–C(6,)–C(7,)	39.4
C(7)–C(4 <sup>*</sup> )–C(5 <sup>*</sup> )–C(6 <sup>*</sup> )	–1.4	C(7,)–C(4, <sup>*</sup> )–C(5, <sup>*</sup> )–C(6, <sup>*</sup> )	3.9

<sup>a</sup> Estimated deviation 1°; the corresponding data were taken from the mirror image of the COD part.

Table 6

Influence <sup>a</sup> of reaction temperature <sup>b</sup> and solvent <sup>c</sup> on the optical yield in hydrogenation of Ph(CH<sub>3</sub>)C=NCH<sub>2</sub>Ph

Temperature (°C)	Optical yield (%)	Composition of solvent (%)		Optical yield (%)
		MeOH	C <sub>6</sub> H <sub>6</sub>	
0	83( <i>R</i> ) <sup>d</sup>	100		73( <i>R</i> )
20	73( <i>R</i> )	80	20	63( <i>R</i> )
40	54( <i>R</i> )	60	40	52( <i>R</i> )
60	44( <i>R</i> )	40	60	39( <i>R</i> )
80	29( <i>R</i> )	20	80	13( <i>R</i> )
100	14( <i>R</i> )		100	6( <i>S</i> )
120	11( <i>S</i> )			
140	20( <i>S</i> )			
160	22( <i>S</i> )			

<sup>a</sup> Reaction conditions: substrate/Rh/P/Et<sub>3</sub>N 100/1/2.2/8; 70 bar H<sub>2</sub>, 6 h, 5 mmol of substrate; conversion: 100%. <sup>b</sup> In methanol, <sup>c</sup> At 20°C. <sup>d</sup> Conversion: 55%.

Table 7

Influence of the solvent composition on the optical yield in hydrogenation of acetophenone <sup>a</sup>

Composition of solvent (%)		Optical yield (%)
MeOH	C <sub>6</sub> H <sub>6</sub>	
100		76( <i>S</i> )
80	20	67( <i>S</i> )
60	40	56( <i>S</i> )
40	60	44( <i>S</i> )
20	80	32( <i>S</i> )
	100	13( <i>S</i> )

<sup>a</sup> Reaction conditions: substrate/Rh/P/Et<sub>3</sub>N 100/1/2.2/2.0; 70 bar H<sub>2</sub>, 50°C, 24 h, 5 mmol of substrate; conversion: 20–70%.

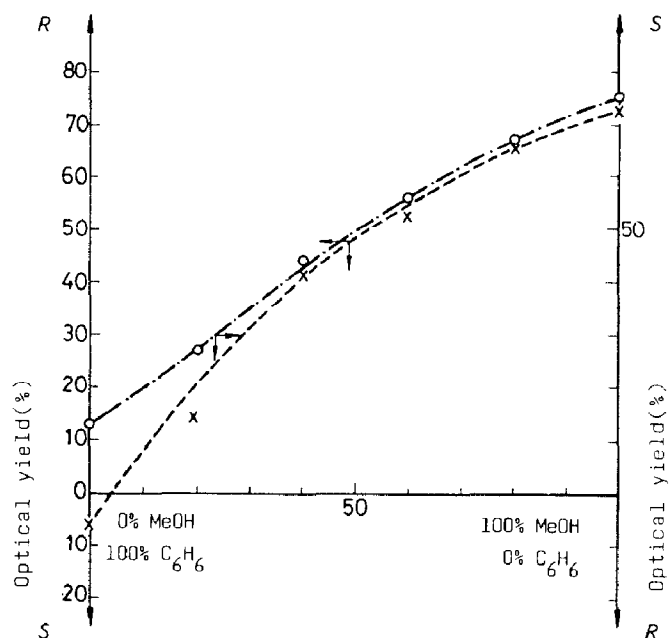


Fig. 4. Solvent dependence of the optical yield in the hydrogenation of acetophenonebenzylimine (x) and acetophenone (O).



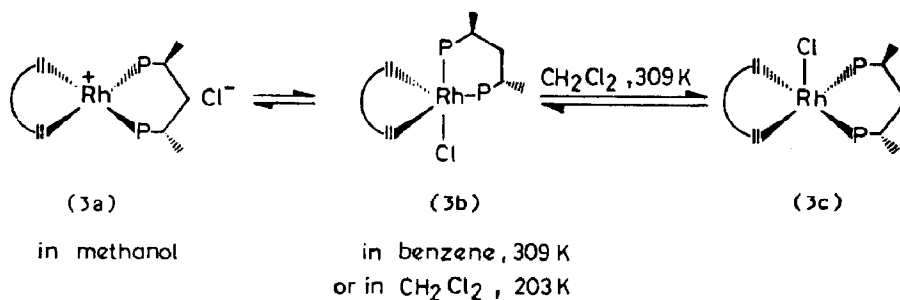


Fig. 5. Structure of Rh((*S,S*)-BDPP)(NBD)Cl (**3**) in various solvents.

composition was observed. Addition of methanol to benzene caused the lines to broaden, and at 0.15% of benzene only a new sharp doublet ( $^1J(\text{RhP})$  131 Hz) is present. Increase in the amount of methanol also resulted in increase in  $^1J(\text{RhP})$ . This suggests that in this mixture square planar (**3a**) and trigonal-bipyramidal (**3b**) complexes are in equilibrium.

The BDPP chelate ring in **3b** has no  $C_2$  symmetry; the two methine protons resonate at substantially different frequencies (a symmetrical septet at 3.87 ppm (6 Hz) (Fig. 6) and a nonet at 2.7 ppm (3–4 Hz)). The corresponding methyl groups give signals at 0.86 ppm and 1.61 ppm, respectively, as sharp doublets of doublets ( $J(\text{PCCH})$  13.7 Hz,  $J(\text{PCCH})$  10.7 Hz,  $J(\text{HCCH})$  7.3 Hz). Since the methylene proton signals overlap with those from an impurity, the vicinal couplings to the methine protons could not be observed directly from the spectrum.

The 400 MHz  $^1\text{H}$  NMR spectra of **1** and **2** in methanol indicate  $C_2$  symmetry for the phosphine chelate ring. The methine protons exhibit a two proton multiplet at 2.94 ppm in **1** (Fig. 6); the methylene protons a first-order multiplet (triplet of triplets,  $^3J(\text{PCCH})$  20.8 Hz,  $^3J(\text{HCCH})$  6.65 Hz) at 1.91 ppm, and the methyl groups a doublet of doublets ( $^3J(\text{PCCH})$  13.5 Hz,  $^3J(\text{HCCH})$  7.0 Hz). The chemical shift of the last signal (1.20 ppm) is close to the mean (1.27 ppm) for the axial and equatorial methyls in **3b**. Consequently the ring probably undergoes interconversion (skew-chair) rapidly on the NMR time scale. In **2** the BDPP protons behave like

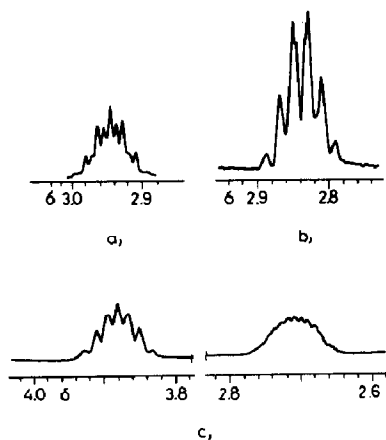


Fig. 6.  $^1\text{H}$  NMR spectra of **1** (a), **2** (b) recorded in  $\text{CD}_3\text{OD}$  and that of **3** (c) recorded in  $\text{C}_6\text{D}_6$  at 293 K. The resonances shown are those for the methine protons of BDPP.

those in **1**, the methyl groups resonating at 1.06 ppm (q,  $^3J(\text{PCCH})$  12.7 Hz;  $^3J(\text{HCCH})$  6.75 Hz), the methines giving a symmetrical multiplet centered at 2.84 ppm, and the methylene protons appearing at 1.76 ppm (regular multiplet), indicating similar symmetry (time-averaged  $C_2$ ) of the rings. These data are consistent with fluxionality of the ring conformation. The fact that the  $J(\text{PCCH})$  value observed for the methyl protons is very close to the mean value of corresponding couplings for **3b** confirms this interpretation.

The spectroscopic evidences outlined above favours a trigonal-bipyramidal structure for **3** with non-equivalent phosphorus atoms and chair chelate conformation in aromatic solvents at room temperature or in  $\text{CH}_2\text{Cl}_2$  at low temperature, and also a conformationally labile ring in square planar complexes independent of the structure of the diene (COD, NBD).

The chirality of rhodium complexes containing (*S,S*)-BDPP is thus extremely sensitive to the solvent. It is reasonable to assume that the formation of chiral  $\delta$ -skew conformation (**IV**) is favorable in methanol, and that the low optical yield in benzene is caused by a quasi-symmetrical chair conformation when acetophenonebenzylimine or acetophenone are hydrogenated.

Although it is known that temperature can strongly influence the enantioselectivity of asymmetric hydrogenation [16–19], the results obtained in the hydrogenation of acetophenonebenzylimine were somewhat unexpected (Table 6). The *R*-enantiomer in the product predominates at lower and the *S*-species at higher temperatures. In order to show the generality of these phenomena we also represent data obtained in asymmetric hydroformylation of styrene with  $\text{PtCl}(\text{SnCl}_3)[(\text{S,S})\text{-BDPP}] + 2 \text{SnCl}_2$  as catalyst [4]. As Fig. 7 shows, there is a strong temperature dependence of the stereoselectivity, and the temperature effect on the rhodium-complex-catalyzed hydrogenation is closely similar to that for the platinum-complex-catalyzed hydroformylation.

The results may be rationalized by taking account of the relative free energies of the diastereomerically activated complexes controlling the asymmetric induction leading to either enantiomer. By considering the possible relationship between the relative free energies of the transition states we can predict the enantioselectivity of the catalyst. It is reasonable to assume that in lower temperature range the chiral  $\delta$ -skew conformation (**IV**) leads to high enantioselectivity. Low induction is expected if the ring is in the achiral chair conformation, with the phenyl rings in achiral array. The prevalence of the opposite enantiomer in higher temperature range can be attributed to the chiral  $\lambda$ -skew conformation (**III**). If steric interactions are the main factors determining the free energies, the substituent would occupy that quadrant in which more space is available, and consequently the  $\delta$ -skew and  $\lambda$ -skew conformations lead to opposite enantiomers [20]. This interpretation involves the assumption that catalytic activity is higher and the proportion lower of the species in which the ring is in a  $\lambda$ -skew conformation.

The similar temperature dependence of the optical yield with (*S,S*)-BDPP-containing catalyst systems in the hydrogenation of acetophenonebenzylimine and in the hydroformylation of styrene and the similar solvent dependence in the hydrogenation of acetophenonebenzylimine and acetophenone, presumably arise from a change in the chelate ring conformation and consequently from the stability of intermediates and kinetic factors. The enhanced flexibility of the ring may be related to the fact that the substrates are simple and free from functional groups,

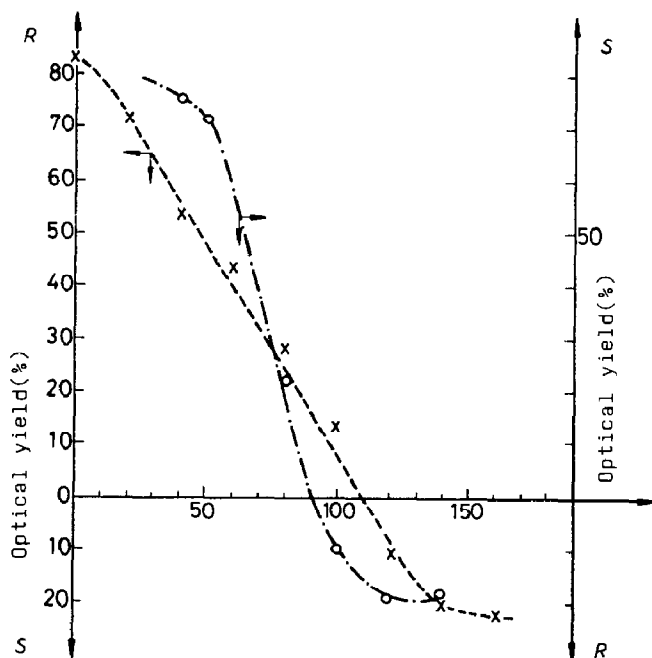


Fig. 7. The temperature dependence of the optical yield in the hydrogenation of acetophenonebenzylamine ( $\times$ ) and in hydroformylation of styrene ( $\circ$ ).

since for functional substrates [3,4] these effects are considerably smaller. The spectroscopic studies of catalytic precursors reveal that steric interactions associated with the whole complex may tip the structural balance in either direction.

## Experimental

All operations were carried out in an inert atmosphere with Schlenk type glassware. Solvents were dried and distilled under argon and degassed before use. Hydrated rhodium(III) chloride was purchased from W.C. Heraeus GmbH. (*S,S*)-BDPP [3],  $[\text{Rh}(\text{NBD})\text{Cl}]_2$  [21] and  $[\text{Rh}(\text{COD})\text{Cl}]_2$  [22] were prepared as previously described. Elemental analyses were performed on a Perkin-Elmer 240.  $^1\text{H}$  NMR spectra were recorded on TESLA BS 487C and Varian XLAA 400,  $^{31}\text{P}$  NMR at 32.1 MHz on a Varian CFT-20. Chemical shifts are given in ppm relative to internal  $\text{Me}_4\text{Si}$  for  $^1\text{H}$  NMR and to external 85%  $\text{H}_3\text{PO}_4$  for  $^{31}\text{P}$  NMR spectra. Chemical shifts downfield from 85%  $\text{H}_3\text{PO}_4$  are defined as positive for the  $^{31}\text{P}$  NMR spectra. The optical rotations of the products were determined on a Schmidt Haensch LM visual polarimeter.

### $[\text{Rh}((-)-(2S,4S)\text{-BDPP})(\text{NBD})]\text{ClO}_4$ (1)

A solution of 965 mg (2.19 mmol) of  $(-)-(2S,4S)\text{-BDPP}$  in 100 ml of methanol was added dropwise to a stirred solution of 461 mg (1.00 mmol) of  $[\text{Rh}(\text{NBD})\text{Cl}]_2$  in 250 ml of methanol. The orange-red solution was stirred for a further 1 h and then treated with a solution of 4.84 g  $\text{NaClO}_4 \cdot \text{H}_2\text{O}$  in 200  $\text{cm}^3$  of deoxygenated water. The red orange precipitate was washed with water and diethyl ether and

dried, to give 645 mg (88%) of product. Anal. Found: C, 56.5; H, 5.2; P, 8.4.  $C_{36}H_{38}P_2ClO_4Rh$  calcd.: C, 58.8; H, 5.2; P, 8.4%.

$^1H$  NMR ( $CD_3OD$ ):  $\delta$  1.19 (dd,  $^3J(PCCH)$  13.5 Hz;  $^3J(HCCH)$  7.0 Hz,  $2CH_3$ ), 1.91 (tr, tr  $^3J(PCCH)$  20.8 Hz,  $^3J(HCCH)$  6.65 Hz,  $CH_2$  in BDPP), 2.94 (m, 2CH), 1.59 (br.s,  $CH_2$  in NBD), 3.95 (nonet,  $J$  1.7 Hz, 2CH in NBD), 4.42 and 4.98 (m, 4CH=), 7.48–7.76 ppm (m, 4 Ph).  $^3P$  NMR:  $\delta$  in  $CDCl_3$  29.8 (d,  $J(RhP)$  149.0 Hz), in  $CD_2Cl_2$  27.3 (d,  $J(RhP)$  149.4 Hz), in  $CD_3OD$  27.5 ppm (d,  $J(RhP)$  149.7 Hz).

*[Rh((-)-(2S,4S)-BDPP)(COD)]ClO<sub>4</sub> (2)*

The procedure described for **1** was used. Anal. Found: C, 58.8; H, 5.6, P, 8.2.  $C_{37}H_{42}P_2ClO_4Rh$  calcd.: C, 59.2; H, 5.6; P, 8.3%.

$^1H$  NMR ( $CD_3OD$ ):  $\delta$  1.06 (q,  $^3J(PCCH)$  12.7 Hz;  $^3J(HCCH)$  6.75 Hz;  $2CH_3$ ), 1.76 (m,  $CH_2$  in BDPP), 2.84 (m, 2CH in BDPP), 2.5–2.65 and 1.9–2.2 (m, 4 $CH_2$  in COD), 4.0 (q,  $^3J(HC=CH) = ^3J(HCCH) = 7.52$  Hz, 2CH=), 4.9 (m, 2CH=) 7.38–8.27 ppm (m, 4Ph).  $^3P$  NMR ( $CDCl_3$ ): 27.8 ppm ( $J(RhP)$  149.0 Hz).  $\Lambda_M$  in MeOH: 86  $ohm^{-1} cm^2 mol^{-1}$ .

Crystals of **1** and **2** suitable for crystal structure determination were grown from methanol solution.

*X-ray structure determination of 1 and 2*

Determination of the unit cell dimensions, space groups, and data collection were performed on a computer-controlled Enraf–Nonius CAD-4 diffractometer at room

Table 8

Crystal data, data collection and least-squares parameters

	1	2
Empirical formula	$C_{36}H_{38}ClO_4P_2Rh$	$C_{37}H_{42}ClO_4P_2Rh$
$M$ (a.m.u.)	735.05	751.05
$F(000)$	756	1552
$a$ (Å)	10.069(1)	14.706(2)
$b$	18.300(2)	13.732(2)
$c$	10.170(1)	20.177(6)
$\beta$ (deg.)	117.22(1)	109.95(2)
$V$ (Å <sup>3</sup> )	1666.4(7)	3830(3)
$Z$	2	4
Space group	$P2_1$	$C2$
$D_c$ ( $g cm^{-3}$ )	1.46	1.30
$\mu$ (Cu-K $\alpha$ )( $cm^{-1}$ )	62.1	54.2
$2\theta$ limits (deg.)		3–150
Scan technique		$\theta-2\theta$
No. of unique reflections	3551	4140
No. of observations ( $NO$ )	3206( $I$ ) $2\sigma(I)$	3893( $I > 3\sigma(I)$ )
Number of variables ( $NV$ )	397	425
Weighting scheme		$4F_0^2\sigma^2(F_0^2)$
$R_0$	0.024	0.041
$R_w$	0.029	0.061
$R_{tot}$	0.037	0.044
$[\Sigma w( F_o  -  F_c )^2 / (NO - NV)]^{1/2}$	1.71	2.60
Rel. transmission $t_{min}$	0.798	0.852
$t_{max}$	1.231	1.701
$t_a$	1.008	1.010

temperature. Details of crystal data, data collection, and least-squares parameters are listed in Table 8.

Structures were solved by the heavy atom (1) and direct methods (2) [23]. All non-hydrogen atoms were refined anisotropically in full-matrix least-squares. At the end of isotropic refinement an empirical absorption correction [24] was applied (Table 8). Hydrogen atoms were placed in calculated positions and were included in the structure factor calculations, but not refined. The absolute configuration of the BDPP used was taken from reference 1.

Programs applied: Enraf-Nonius SDP-Plus [25], and local programs on a PDP 11/34 minicomputer (128 kw). The atomic coordinates are listed in Tables 1 and 3, and selected bond lengths and bond angles in Tables 2 and 4. Tables of anisotropic thermal parameters, H atom coordinates, and lists of calculated and observed structure factors are available from the authors.

### *Rh((-)-(2S,4S)-BDPP)(NBD)Cl (3)*

The complex was characterized by  $^1\text{H}$  and  $^{31}\text{P}$  NMR after its formation in situ from the reaction of  $[\text{Rh}(\text{NBD})\text{Cl}]_2$  and (*S,S*)-BDPP.

$^1\text{H}$  NMR ( $\text{C}_6\text{D}_6$ ):  $\delta$  0.86 and 1.61 (dd,  $^3J(\text{PCCH})$  13.7 Hz,  $^3J(\text{HCCH})$  7.3 Hz,  $2\text{CH}_3$ ), 1.28–1.53 (m,  $\text{CH}_2$  in BDPP), 2.7 (nonet,  $J$  3–4 Hz,  $\text{CH}_{\text{eq}}$ , 3.87 (hept.,  $J$  6 Hz,  $\text{CH}_{\text{ax}}$ ), 0.93 (br.s,  $\text{CH}_2$  in NBD), 3.13 (m,  $2\text{CH}=\text{}$ ), 3.71 (q,  $J$  3.7 Hz,  $2\text{CH}=\text{}$ ), 3.32 ppm (nonet,  $2\text{CH}$  in NBD), 6.82–7.85 ppm (m, 4Ph).  $^{31}\text{P}$  NMR:  $\delta$  in  $\text{C}_6\text{D}_6$  12.2 (dd,  $^1J(\text{RhP})$  130 Hz,  $^2J(\text{P}^1\text{P}^2)$  60 Hz, P), 39.3 (dd,  $^1J(\text{RhP})$  132 Hz,  $^2J(\text{P}^2\text{P}^1)$  60 Hz,  $\text{P}^2$ ), in  $\text{CD}_2\text{Cl}_2$  25.3 ppm (d,  $^2J(\text{RhP})$  1.33 Hz).  $\Delta$ : 0.04 in  $\text{C}_6\text{H}_6$ , 1.7 in  $\text{CH}_2\text{Cl}_2$  and  $66 \text{ ohm}^{-1} \text{ cm}^2 \text{ mol}^{-1}$  in MeOH.

### *Hydrogenation experiments*

In a typical experiment, appropriate amounts of (*S,S*)-BDPP and  $[\text{Rh}(\text{NBD})\text{Cl}]_2$  were dissolved in  $10 \text{ cm}^3$  of solvent under argon. The solution was prehydrogenated for 40 min at room temperature. The substrate (5 mmol) and the prehydrogenated solution were injected into a 20 ml stainless steel autoclave.

The hydrogenations were performed under the conditions given in Tables 6 and 7. Products obtained from hydrogenations of acetophenone and acetophenonebenzylimine were separated from the catalyst by distillation. Conversion were determined by GLC. The optical yields were calculated by use of reported values for the optical rotations of the pure products [26,27]. In some cases the optical yields were determined by using the optically active NMR shift reagents, tris(3-(heptafluoropropylhydroxymethylene)-*d*-camphoratoeuropium(III) for 1-phenylethanol and tris(*d,d*-dicampholymethanato)europium(III) for *N*-( $\alpha$ -methylbenzyl)-benzylamine, respectively. The optical purities so obtained were in excellent agreement with those derived from rotation values.

### References

- 1 P.A. MacNeil, N.K. Roberts and B. Bosnich, *J. Am. Chem. Soc.*, 103 (1981) 2273.
- 2 J. Bakos, I. Tóth and L. Markó, *J. Org. Chem.*, 46 (1981) 5427.
- 3 J. Bakos, I. Tóth, B. Heil and L. Markó, *J. Organomet. Chem.*, 279 (1985) 23.
- 4 L. Kollár, J. Bakos, I. Tóth and B. Heil, *J. Organomet. Chem.*, 350 (1988) 277.
- 5 M.D. Fryzuk, B. Bosnich, *J. Am. Chem. Soc.*, 99 (1977) 6262.
- 6 M.D. Fryzuk, B. Bosnich, *J. Am. Chem. Soc.*, 101 (1979) 3043.

- 7 H. Boucher, B. Bosnich, *Inorg. Chem.*, 15 (1976) 1471.
- 8 M. Kojima, M. Fujita, F. Fujita, *Bull. Chem. Soc. Jpn.*, 50 (1977) 898.
- 9 M. Kojima, J. Fujita, *Bull. Chem. Soc. Jpn.*, 50 (1977) 3237.
- 10 M. Goto, N. Nakayabu, H. Ito, H. Tsubamoto, K. Nakabayashi, Y. Kuroda and T. Sakai, *Inorg. Chem.*, 25 (1986) 1684.
- 11 L.J. DeHayes, D.H. Busch, *Inorg. Chem.*, 12 (1973) 1505.
- 12 S.R. Niketic, F. Woldbye, *Acta Chem. Scand.*, 27 (1973) 621.
- 13 H.B. Kagan, in G. Wilkinson, F.G.A. Stone (Eds.), *Comprehensive Organometallic Chemistry*, Pergamon, Oxford, Vol. 8, 1982, p. 463–498.
- 14 B. Bosnich, M.D. Fryzuk, *Top. Stereochem.*, 12 (1981) 119.
- 15 W.S. Knowles, W.S. Christophel, K.E. Koenig, C.F. Hobbs, *Adv. Chem. Ser.*, 196 (1982) 325.
- 16 I. Ojima, T. Kogure, N. Yoda, *J. Org. Chem.*, 45 (1980) 4728.
- 17 D. Sinou, *Tetrahedron Lett.*, 22 (1981) 2987.
- 18 W.S. Knowles, M.J. Sabacky, B.D. Vineyard, *Adv. Chem. Ser.*, 132 (1974) 274.
- 19 C.L. Landis and J. Halpern, *J. Am. Chem. Soc.*, 109 (1987) 1746.
- 20 G. Consiglio and P. Pino, *Adv. Chem. Ser.*, 196 (1982) 371.
- 21 E.W. Abel, M.A. Bennett and G. Wilkinson, *J. Chem. Soc.*, (1959) 3178.
- 22 J. Chatt and L.M. Venanzi, *J. Chem. Soc. A*, (1957) 4735.
- 23 P. Main, S.E. Hull, L. Lessinger, G. Germain, J.-P. Declercq and M.M. Woolfson, *MULTAN 82. A System of Computer Programs for the Automatic Solution of Crystal Structures from X-ray Diffraction Data*, Univs. of York, England, and Louvain, Belgium.
- 24 N. Walker and D. Stuart, *Acta Crystallogr. A*, 39 (1983) 158.
- 25 B.A. Frenz, *The Enraf–Nonius CAD-4 Structure Determination Package*. Enraf–Nonius, Delft, The Netherlands, 1983.
- 26 K. Parkc, *J. Prakt. Chem.*, 86 (1912) 387.
- 27 U. Nagai, T. Shishido, R. Chiba, H. Mitsuhashi, *Tetrahedron*, 21 (1965) 1701.